

## PDF hosted at the Radboud Repository of the Radboud University Nijmegen

The following full text is a preprint version which may differ from the publisher's version.

For additional information about this publication click this link.

<http://hdl.handle.net/2066/92442>

Please be advised that this information was generated on 2020-10-22 and may be subject to change.

# The binary companion of PSR J1740–3052

C. G. Bassa<sup>1\*</sup>, W. F. Brisken<sup>2</sup>, G. Nelemans<sup>3</sup>, I. H. Stairs<sup>4</sup>, B. W. Stappers<sup>1</sup>, M. Kramer<sup>5,1</sup>

<sup>1</sup>*Jodrell Bank Centre for Astrophysics, The University of Manchester, Manchester, M13 9PL, United Kingdom*

<sup>2</sup>*National Radio Astronomy Observatory, Socorro, NM 87801, USA*

<sup>3</sup>*Department of Astrophysics, IMAPP, Radboud University Nijmegen, Toernooiveld 1, 6525 ED, Nijmegen, The Netherlands*

<sup>4</sup>*Department of Physics and Astronomy, University of British Columbia, 6224 Agricultural Road, Vancouver BC V6T 1Z1, Canada*

<sup>5</sup>*Max Planck Institut für Radioastronomie, Auf dem Hügel 69, 53121 Bonn, Germany*

Accepted 2010 December 20. Received 2010 December 15; in original form 2010 November 12

## ABSTRACT

We report on the identification of a near-infrared counterpart to the massive ( $> 11 M_{\odot}$ ) binary companion of pulsar J1740–3052. An accurate celestial position of PSR J1740–3052 is determined from interferometric radio observations. Adaptive optics corrected near-infrared imaging observations show a counterpart at the interferometric position of the pulsar. The counterpart has  $K_s = 15.87 \pm 0.10$  and  $J - K_s > 0.83$ . Based on distance and absorption estimates from models of the Galactic electron and dust distributions these observed magnitudes are consistent with those of a main-sequence star as the binary companion. We argue that this counterpart is the binary companion to PSR J1740–3052 and thus rule out a stellar mass black hole as the pulsar companion.

**Key words:** binaries: general – stars: early-type – pulsars: general – pulsars: individual: PSR J1740–3052 – infrared: stars – astrometry

## 1 INTRODUCTION

Among the radio pulsars that are found in binary systems, four belong to a subgroup where the pulsar has the characteristics of a young, isolated pulsar, but is orbiting a massive companion ( $\gtrsim 3 M_{\odot}$ ) in a rather wide (50–2000 day orbital period) and eccentric ( $e > 0.5$ ) orbit (Stairs 2004; van Kerkwijk et al. 2005). The companion to the first of these systems, PSR B1259–63 (Johnston et al. 1992) was identified as a  $V = 10$  early-type B2e star. PSR J0045–7319, located in the SMC, is the second system and has a  $V = 16$  B1 V companion (Kaspi et al. 1994). No information on a possible counterpart has been published for the fourth system, PSR J1638–4725 (Lorimer et al. 2006).

The third system, PSR J1740–3052, was discovered by Stairs et al. (2001) in the Parkes Multibeam Survey (Manchester et al. 2001) as a young (350 kyr) pulsar. Subsequent timing observations showed that the pulsar is part of a binary system with an orbital period of 231 d and an eccentricity of 0.57. The mass function of the pulsar yielded a lower limit to the mass of the companion of  $11 M_{\odot}$ . A candidate counterpart to PSR J1740–3052 was identified in near-infrared observations. From  $K$ -band spectra, the counterpart was classified as late-type, having a spectral type between K5 and M3 (Stairs et al. 2001). This identification is at odds with the binary parameters which set the Roche

lobe radius significantly smaller than that expected for a late-type star at the estimated distance. Subsequent phase-resolved spectroscopic observations by Tam et al. (2010) confirmed the unlikelihood of the star being the binary companion, as no significant radial velocity variations consistent with the expected binary orbit were found.

The nature of the massive binary companion remains unclear, and could be either an early-type main-sequence star or a compact remnant. Though Stairs et al. (2001) reported small variations in the dispersion measure of PSR J1740–3052 near periastron, which would be consistent with a stellar companion, they could not conclusively rule out a stellar mass black hole as the binary companion.

In this paper we report on interferometric radio observations to obtain an accurate position of the PSR J1740–3052 and adaptive optics corrected near-infrared observations to search for a stellar counterpart to PSR J1740–3052. Section 2 describes the interferometric observations, while Section 3 details the astrometry and photometry of the near-infrared imaging. We discuss the results in Section 4 and conclude in Section 5.

## 2 RADIO OBSERVATIONS

The NRAO Very Large Array (VLA) was used to determine the position of the pulsar under project code AS769. The observation was made over a 5 h period starting at UTC 23:19

\* email: bassa@jb.man.ac.uk

on September 3rd, 2003 using the VLA in its most extended A-configuration. This observation included the Pie Town antenna for even greater East-West resolution. Spectral line mode mode 2AC was used to provide 25 MHz of bandwidth centered at 1678.4 MHz on each circular polarization. The correlator integration time was set to 5 s. The observation consisted of a 600 s observation of 3C286 followed by 14 loops containing three sources: 90 s on PMN J1751–2524, 90 s on PMN J1820–2528 and 930 s on PSR J1740–3052.

Data reduction was performed within AIPS in a standard manner. Flux density and bandpass calibration were performed on 3C286. Calibrator source PMN J1751–2524 was used as the position reference. Its assumed position was taken to be  $\alpha_{J2000} = 17^{\text{h}}51^{\text{m}}51^{\text{s}}.2630$ ,  $\delta_{J2000} = -25^{\circ}24'00''.060$  (Fey et al. 2004). Phases and amplitudes determined on this source were applied to PMN J1820–2528 and PSR J1740–3052. Imaging was performed using the robust weighting factor of unity as a compromise between resolution and sensitivity; the resultant beam size was  $0''.91 \times 2''.17$  oriented  $2^{\circ}$  East of North. Wide-field imaging of the PSR J1740–3052 data was performed in order to clean side-lobes from numerous bright sources over the entire  $25'$  field of view. Most notably, the  $5'$  diameter object known as *The Tornado* (see Gaensler et al. 2003 and references within), is only  $8.1$  Southwest of the pulsar. Due to the lack of short interferometer spacings, the ability to model and clean this source well was limited. Fortunately the pulsar lies outside the worst side-lobes which emanate mostly North and South from the object. The pulsar was detected less than one beam-width from the position reported by Stairs et al. (2001) with a flux density of  $0.26 \pm 0.04$  mJy. Despite the best effort to clean the side-lobes of confusing sources, the pulsar was found on top of residual large scale structure. In order to fit the position of the pulsar, linear flux density slices were made along the right ascension and declination axes through the center of the detected pulsar. Each of these two slices were then fit for a 1-D Gaussian and an underlying linear gradient. The resultant best fit position of the pulsar is  $\alpha_{J2000} = 17^{\text{h}}40^{\text{m}}50^{\text{s}}.001$ ,  $\delta_{J2000} = -30^{\circ}52'04''.30$ . The  $1\sigma$  uncertainties on this position are  $0''.069$  in right ascension and  $0''.21$  in declination. The effect of an incorrectly modeled underlying gradient was found to result in deflections much smaller than the fit uncertainty so are not considered. The final uncertainty reported above is entirely due to measurement error.

The 0.8 Jy VLA calibrator source PMN J1820–2528 has nearly the same angular separation ( $6''.6$ ) from the calibrator source PMN J1751–2524 as does PSR J1740–3052 ( $6''.0$ ) and was used as an astrometric check source. It was imaged using the same parameters as used for PSR J1740–3052. Its fit position ( $\alpha_{J2000} = 18^{\text{h}}20^{\text{m}}57^{\text{s}}.84909$ ,  $\delta_{J2000} = -25^{\circ}28'12''.5403$ ) differed from its cataloged position ( $\alpha_{J2000} = 18^{\text{h}}20^{\text{m}}57^{\text{s}}.8486$ ,  $\delta_{J2000} = -25^{\circ}28'12''.584$ ; Fey et al. 2004) in each axis by an amount much smaller than the statistical uncertainty of the pulsar position.

### 3 INFRARED OBSERVATIONS

Adaptive optics corrected near-infrared imaging of the field containing PSR J1740–3052 was obtained with NACO (NAOS-CONICA; Lenzen et al. 2003; Rousset et al. 2003)

at the ESO Very Large Telescope on Paranal, Chile in July and August of 2006. A log of the observations is given in Table 1. Images were obtained in the  $J$ ,  $H$  and  $K_s$ -bands using the S27 camera, which provides a  $1\text{k} \times 1\text{k}$  chip with a  $0''.027 \text{ pix}^{-1}$  pixel scale yielding a  $28'' \times 28''$  field-of-view. The late-type candidate counterpart of Stairs et al. (2001) was used as a natural guide star for the wavefront sensor which corrects the atmospheric distortions in the incoming wavefront. The N90C10 dichroic was used for  $K_s$  observations, while the K dichroic was used for  $J$  and  $H$ -band imaging. The dithered NACO observations were used to create a sky frame containing the contribution of both the dark current and the inhomogeneities in the sky for each filter and exposure time combination. After subtraction of this sky frame, the science frames were registered using integer pixel offsets and averaged.

Our aim was to obtain an accurate absolute astrometric calibration of the NACO images using the USNO CCD Astrograph Catalog (UCAC3; Zacharias et al. 2010) to allow comparison with the interferometric pulsar position. The positional uncertainties of the standards in this catalog are 20 mas for stars with  $R \lesssim 14$  and 70 mas for  $R \lesssim 16$ , but with 1.3 stars per square arc-minute the star density in the direction of PSR J1740–3052 is low and none of the standards coincides with the NACO field-of-view.

In order to allow calibration against the UCAC3 catalog, imaging observations were obtained with two further instruments. Narrow-band near-infrared images at 1.19 and  $2.25 \mu\text{m}$  were taken with ISAAC (Moorwood et al. 1998), also at the VLT in June 2006. The total exposure times were 936 s and 800 s respectively. This instrument has a  $1\text{k} \times 1\text{k}$  CCD with a  $0''.148 \text{ pix}^{-1}$  pixel scale with a  $2'.5 \times 2'.5$  field-of-view. The observations were corrected for dark current and flat-field effects and registered and averaged using standard routines. Finally,  $R$ ,  $I$  and  $z$ -band images were obtained with the Wide Field Imager (WFI; Baade et al. 1999) at the 2.2 m ESO telescope on La Silla, Chile in August 2006. This instrument is a mosaic of  $8 \text{ k} \times 4 \text{ k}$  CCDs each with a pixel size of  $0''.238 \text{ pix}^{-1}$  and a  $8' \times 16'$  field-of-view. We only use the data from the CCD that contains the pulsar location. Bias-subtraction and flat-fielding were performed using standard routines. The  $I$  and  $z$ -band images were further corrected for fringe frames which were constructed from the dithered science observations. All data reduction was done using the Munich Image Data Analysis System (MIDAS).

Stars on an  $8' \times 8'$  subsection of a 45 s  $R$ -band WFI image were compared to UCAC3 standards. A total of 79 astrometric standards coincided with the image, of which 72 were not saturated and appeared stellar and unblended. An astrometric solution was determined by fitting for position and a four parameter transformation matrix. By iteratively removing outliers the solution converged using 67 standards providing rms residuals of  $0''.073$  in right ascension and  $0.070$  in declination.

This astrometric solution was transferred from the WFI image to the NACO images by using the  $1.19 \mu\text{m}$  and  $2.25 \mu\text{m}$  ISAAC images to generate tertiary and quaternary astrometric catalogs. Pixel positions on the ISAAC images were corrected for geometric distortion using the May 2005

**Table 1.** NACO Observation log. The columns give the date and time of the observations, the integration time  $t_{\text{int}}$ , the filter used, the observed FWHM  $\sigma$  of the stellar profiles and the observed magnitude or limit on the magnitude in this filter used.

Date & Time (UT)	$t_{\text{int}}$ (s)	Filter	$\sigma$	Mag.
July 13	04:11–05:03	$195 \times 10$	$K_s$	$0''.13$ 15.87
	05:43–05:52	$50 \times 5$	$H$	$0''.21$ > 15.1
	05:55–06:57	$47 \times 50$	$J$	$0''.36$ > 16.7
August 14	00:03–00:50	$31 \times 50$	$K_s$	$0''.25$ > 12.8
August 21	00:13–00:22	$50 \times 5$	$H$	$0''.25$ > 14.1
	00:25–01:26	$240 \times 10$	$J$	$0''.39$ > 16.1
	01:29–02:00	$48 \times 25$	$K_s$	$0''.20$ > 13.5

transformation provided by ESO<sup>1</sup>. The transfer of the astrometric solution from the  $R$ -band WFI image to the  $1.19 \mu\text{m}$  ISAAC image used 56 stars, providing rms residuals of  $0''.022$  in right ascension and  $0''.023$  in declination. The solution was then transferred to the  $2.25 \mu\text{m}$  image, using 120 stars yielding rms residuals of  $0''.012$  in right ascension and  $0''.011$  in declination. Finally, 29 stars were used to transfer the solution to the NACO  $K_s$ -band image obtained on July 13. The residuals of the transfer were  $0''.012$  in right ascension and  $0''.016$  in declination.

The total uncertainty in the astrometry of the NACO image is the quadratic sum of the uncertainties in the astrometric solutions, which amount to  $0''.078$  in right ascension and  $0''.076$  in declination and is dominated by the uncertainties in the calibration of the WFI image by the UCAC3 catalog. Even though multiple transfers of the astrometric solution are needed, it is still more accurate than the direct calibration of the  $2.25 \mu\text{m}$  ISAAC image using 160 stars from the 2MASS catalog (Skrutskie et al. 2006), which yields residuals of  $0''.11$  in both coordinates.

Combined with the uncertainty of the interferometric position of PSR J1740–3052 the 95% confidence region on the NACO images is an ellipse with a semi-minor axis of  $0''.26$  in right ascension and a semi-major axis of  $0''.55$  in declination. This confidence region is shown in Fig. 1 and is located  $0''.18$  West and  $0''.37$  South of the late-type star, which itself is located just inside the 95% confidence region. Inspection of the NACO images shows that the July 13th, 2006  $K_s$ -band image contains a star located inside the error ellipse, see Fig. 2. The position of the counterpart in that image is  $\alpha_{J2000} = 17^{\text{h}}40^{\text{m}}50^{\text{s}}.001 \pm 0^{\text{s}}.006$  and  $\delta_{J2000} = -30^{\circ}52'04''.27 \pm 0''.08$ , which is offset from the interferometric position of PSR J1740–3052 by  $0''.00 \pm 0''.10$  in right ascension and  $0''.03 \pm 0''.22$  in declination. Based on the stellar density of the  $K_s$ -band image, we estimate that the probability of finding a random star this close to the interferometric position of PSR J1740–3052 is only 0.05 per cent.

Point-spread-function (PSF) photometry was performed on the averaged NACO images using DAOPHOT II (Stetson 1987) running within MIDAS. An analytical Moffat profile (Moffat 1969) with a fixed exponent of  $\beta = 2.5$  combined with an empirical look-up table was used to represent the PSF. The parameters of the PSF were kept constant

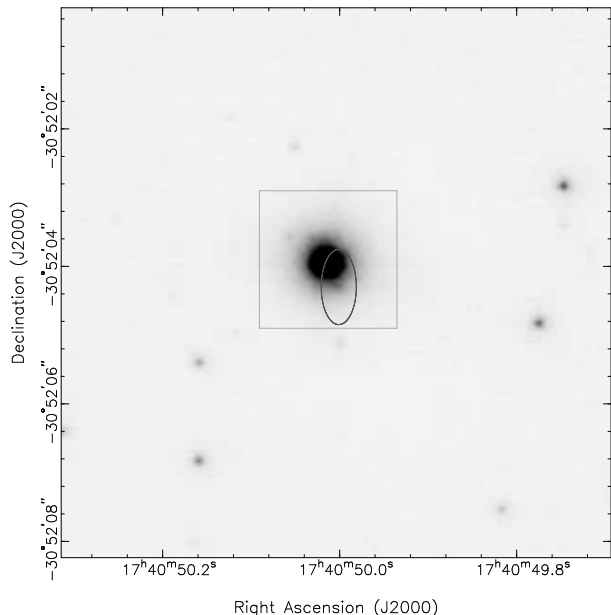


**Figure 1.** A  $8'' \times 8''$  subsection of the  $K_s$ -band images obtained with NACO on July 13th, 2006. The ellipse denotes the 95% confidence error region of the interferometric radio position of the pulsar. The bright star near the center is the late-type star which Tam et al. (2010) showed is unlikely to be the binary companion to PSR J1740–3052. This star is located on the edge of the error region. Only a fainter star is present in the error ellipse. The  $2'' \times 2''$  box is the field shown in Fig. 2.

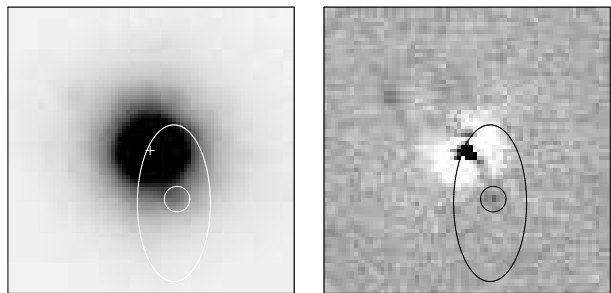


**Figure 2.** A  $2'' \times 2''$  subsection of Fig. 1 centered on the bright late-type star, showing the original image and with the stellar profile of the late-type star subtracted. Some artifacts from the late-type star are still present due to imperfect definition of the point-spread-function. The ellipse denotes the 95% confidence error region on the interferometric position of PSR J1740–3052. The counterpart to PSR J1740–3052 is encircled in both panels.

over the image. Due to the low apparent stellar density on the NACO images, the majority of the stars on the images were used to determine the PSF.

The instrumental  $JHK_s$  PSF magnitudes were calibrated against values from the 2MASS catalog (Skrutskie et al. 2006). Due to the small field-of-view of NACO, 4 stars were used to determine zero-point magnitude offsets. No color terms were fitted for. The rms residuals of the fits were 0.09 mag in  $J$ -band and 0.06 mag in both  $H$  and  $K_s$ .

The counterpart to PSR J1740–3052 is detected in the July 13th  $K_s$ -band image, where it has  $K_s = 15.87 \pm 0.10$ . Limits on the magnitude of the counterpart in the other images were determined using simulations. For each image

<sup>1</sup> [http://www.eso.org/sci/facilities/paranal/instruments/isaac/inst/field\\_distortion.html](http://www.eso.org/sci/facilities/paranal/instruments/isaac/inst/field_distortion.html)

a set of copies were generated where an artificial star of a certain magnitude was placed on the position of the counterpart. Each of these copies was then photometered using the same routines as the original. The  $3\sigma$  detection limit was set when the artificial star was recovered with a signal-to-noise of 3. The limiting magnitudes are given in Table 1. The most stringent limits set  $J > 16.7$  and  $H > 15.1$ .

#### 4 DISCUSSION

We will now use the  $K_s$ -band detection and  $J$  and  $H$ -band non-detections of the counterpart and compare them with values predicted for the companion of PSR J1740–3052.

The radio timing observations by Stairs et al. (2001) place several constraints on the properties of the companion. Assuming the pulsar has a canonical mass of  $1.4 M_\odot$ , the measurements of the orbital period and semi-major axis limit the mass of the companion to  $M_c > 11 M_\odot$ . The radius of the companion is constrained by the radius of the Roche lobe at the periastron distance of the orbit. A further upper limit on the radius is set by the lack of eclipses of the pulsar seen in the radio observations. Figure 3 shows these constraints. Assuming the magnetic field of the pulsar is a dipole, the rotational properties of the pulsar can be used to determine the age of the pulsar. For PSR J1740–3052 this characteristic age is 350 kyr, and binary evolution dictates that the companion must be older than that, as the prior evolution of the pulsar progenitor must be involved (Tauris & van den Heuvel 2006).

At a Galactic longitude of  $l = 357^\circ.81$  and latitude of  $b = -0^\circ.13$ , PSR J1740–3052 is located only  $2^\circ.2$  from the Galactic Center, and hence the electron and dust column densities are substantial. At a dispersion measure (DM) of  $740.9 \text{ cm}^{-3} \text{ pc}^{-1}$  (Stairs et al. 2001), PSR J1740–3052 is one of the pulsars with the largest DM. For its line-of-sight, distance estimates from models of the Galactic electron density distribution based on the observed DM range from 8 to 14 kpc (Taylor & Cordes 1993) and 6.3 to 11 kpc (Cordes & Lazio 2002).

The COBE dust maps by Schlegel et al. (1998) set the maximum reddening for this line-of-sight at  $E_{B-V} = 18$ . Using the Schlegel et al. (1998) relative extinction coefficients, this is equivalent to a maximum  $V$  and  $K_s$ -band absorption of  $A_V \lesssim 59$  and  $A_K \lesssim 6.7$ . The nearest distinct line-of-sight of the Galactic extinction model by Marshall et al. (2006) is within  $8'$  of PSR J1740–3052 and estimates  $K_s$ -band absorption of  $A_K = 1.9$  at a distance of 5.0 kpc, up to  $A_K = 2.5$  at 10.4 kpc. This model determines the extinction distribution by comparing 2MASS observations with predictions of a Galactic stellar population synthesis model (Robin et al. 2003). For comparison, the Galactic extinction model by Drimmel et al. (2003), where red clump stars in the 2MASS observations are used to derive distance dependent extinction, estimates  $A_K$  of 1.2 at 5.0 kpc, 1.7 at 10 kpc and 3.0 at 15 kpc. Hence, based on the observed  $K_s$ -band magnitude of the counterpart and a conservative estimate on the range of distances ( $d = 5$  to 15 kpc) and absorptions ( $A_K = 1.2$  to 3.0), the absolute  $K_s$ -band magnitude of the counterpart falls in the range of  $M_K = 1.2$  to  $-3.0$ .

Stellar isochrones by Marigo et al. (2008) show that main-sequence stars have  $M_J - M_K = (J - K_s)_0 > -0.25$ .

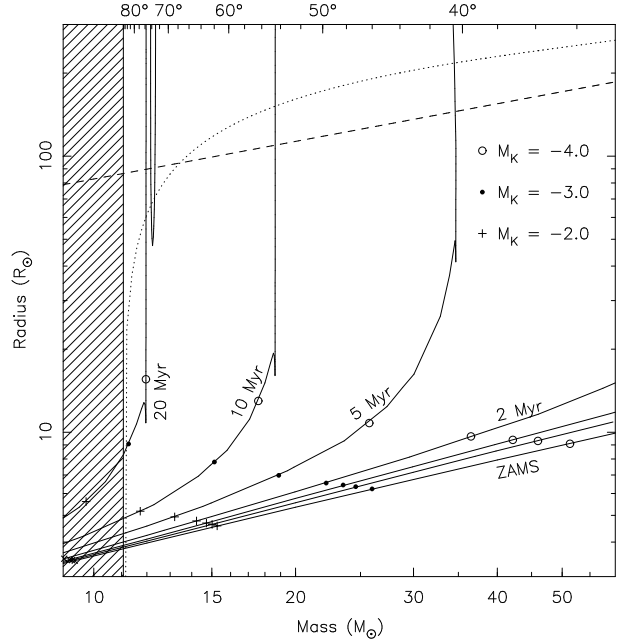


**Figure 3.** Constraints on the properties of the binary companion of PSR J1740–3052. Assuming a canonical pulsar mass of  $1.4 M_\odot$ , the orbital parameters measured by Stairs et al. (2001) limit the companion to a mass of  $M_c > 11 M_\odot$ . The Roche lobe radius at periastron is shown with the dashed line, setting an upper limit to the companion radius. A further upper limit, shown with the dotted line, on the companion radius is set by the absence of eclipses of the radio signal. Stars with radii larger than this limit would eclipse the pulsar when it passes the line-of-sight. Stellar isochrones from the Padova models by Marigo et al. (2008) are shown with the solid lines, ranging from zero-age main-sequence models to models at ages of 0.5, 1, 2, 5, 10 and 20 Myr. Each isochrone shows the location where the star reaches absolute  $K_s$ -band magnitudes of  $M_k = -2$ ,  $-3$  and  $-4$ . The observed range of  $1.2 > M_K > -3.0$  shows that the companion is on the main-sequence.

Hence the observed limit on  $J - K_s > 0.83$  limits the  $J - K_s$  reddening to  $E_{J-K} > 1.08$ . Using the Schlegel et al. (1998) extinction coefficients this sets  $A_K > 0.74$ , which is consistent with the estimates from Galactic absorption models. The observed limit on  $H - K_s$  does not provide a better constraint.

Figure 3 shows the predictions for mass and radius of the Marigo et al. (2008) isochrones. They show that zero-age main-sequence stars with masses up to  $25 M_\odot$  will have absolute  $K_s$ -band magnitudes that satisfy the observed range of  $M_K = 1.2$  to  $-3.0$ . Less massive but more evolved main-sequence stars up to ages of 20 Myr at  $11 M_\odot$  also satisfy this range. The constraints on the mass and brightness of the companion of PSR J1740–3052 show that the companion must be on the main-sequence. Furthermore, since the isochrones predict that main-sequence stars more massive than  $11 M_\odot$  have  $M_K \lesssim -1.5$  the  $K_s$ -band distance modulus must be larger than  $(m - M)_K > 17.4$ , which suggests PSR J1740–3052 is located at the far end of the distance ranges estimated from Galactic electron density models.

## 5 CONCLUSIONS

Since its discovery, it was unclear if the binary companion of PSR J1740–3052 was an early-type main-sequence star, a late-type giant, or a stellar mass black hole, though the data favored a main-sequence type companion. Using accurate astrometric radio interferometry and adaptive optics corrected near-infrared imaging observations, we show that the late-type star located near the pulsar position is located at the edge of the 95% confidence error ellipse of the interferometric radio position of the pulsar. This further strengthens the case made by Stairs et al. (2001) and Tam et al. (2010) that it is not the binary companion to PSR J1740–3052.

In the wings of the late-type star, and near the center of the error ellipse, we find a counterpart whose observed  $K_s$ -band magnitude is consistent with the expected mass and age of the binary companion to PSR J1740–3052 at the estimated distance and reddening to the system. We argue that this counterpart is the binary companion to PSR J1740–3052. Our observations show that the companion is on the main-sequence, which is consistent with the observations of both the small variations in the dispersion measure near periastron of the binary orbit, and the periastron advance being due to tidal and spin quadrupoles (Stairs et al. 2001). These observations rule out the need for a black hole or a giant as the binary companion.

At  $K_s = 15.87$  the companion is within reach of near-infrared spectrographs. Adaptive optics would be a necessity to resolve the companion in the wings of the late-type star which is almost 6 mag brighter in  $K_s$ . To extract the spectrum of the companion an algorithm such as that of Hynes (2002) would be needed to resolve the blend. Spectra of the companion could be used to further confirm the identification through radial velocity variations and the spectral classification.

With a massive main-sequence companion, the PSR J1740–3052 system likely experienced a previous phase of mass transfer in which the progenitor of the pulsar lost its hydrogen envelope and the companion accreted a significant amount of mass (for a review, see Tauris & van den Heuvel 2006). The subsequent (type Ib) supernova caused the orbit to become eccentric. In the next few million years the companion will evolve off the main-sequence and tidal forces will circularize the orbit when the star approaches Roche lobe overflow. The ensuing common envelope phase will likely lead to a merger and the formation of a Thorne-Zytkow object (Thorne & Zytkow 1975) as there is not enough energy in the orbit to unbind the envelope of the subgiant (e.g. Deloye & Taam 2010).

## ACKNOWLEDGMENTS

The National Radio Astronomy Observatory (NRAO) is a facility of the National Science Foundation operated under cooperative agreement by Associated Universities, Inc. This research is based on observations made with ESO Telescopes at the La Silla or Paranal Observatories under program ID 077.D-0683. Pulsar research at UBC is supported by an NSERC Discovery Grant.

## REFERENCES

- Baade D., Meisenheimer K., Iwert O., et al. 1999, *The Messenger*, 95, 15
- Cordes J. M., Lazio T. J. W., 2002, [astro-ph/0207156](#)
- Deloye C. J., Taam R. E., 2010, *ApJ*, 719, L28
- Drimmel R., Cabrera-Lavers A., López-Corredoira M., 2003, *A&A*, 409, 205
- Fey A. L., Ma C., Arias E. F., Charlot P., Feissel-Vernier M., Gontier A., Jacobs C. S., Li J., MacMillan D. S., 2004, *AJ*, 127, 3587
- Gaensler B. M., Fogel J. K. J., Slane P. O., Miller J. M., Wijnands R., Eikenberry S. S., Lewin W. H. G., 2003, *ApJ*, 594, L35
- Hynes R. I., 2002, *A&A*, 382, 752
- Johnston S., Manchester R. N., Lyne A. G., Bailes M., Kaspi V. M., Qiao G., D’Amico N., 1992, *ApJ*, 387, L37
- Kaspi V. M., Johnston S., Bell J. F., Manchester R. N., Bailes M., Bessell M., Lyne A. G., D’Amico N., 1994, *ApJ*, 423, L43
- Lenzen R., Hartung M., Brandner W., et al. 2003, in M. Iye & A. F. M. Moorwood ed., *Society of Photo-Optical Instrumentation Engineers (SPIE) Conference Series Vol. 4841 of Society of Photo-Optical Instrumentation Engineers (SPIE) Conference Series, NAOS-CONICA first on sky results in a variety of observing modes*. pp 944–952
- Lorimer D. R., Faulkner A. J., Lyne A. G., Manchester R. N., Kramer M., McLaughlin M. A., Hobbs G., Possenti A., Stairs I. H., Camilo F., Burgay M., D’Amico N., Corongiu A., Crawford F., 2006, *MNRAS*, 372, 777
- Manchester R. N., Lyne A. G., Camilo F., Bell J. F., Kaspi V. M., D’Amico N., McKay N. P. F., Crawford F., Stairs I. H., Possenti A., Kramer M., Sheppard D. C., 2001, *MNRAS*, 328, 17
- Marigo P., Girardi L., Bressan A., Groenewegen M. A. T., Silva L., Granato G. L., 2008, *A&A*, 482, 883
- Marshall D. J., Robin A. C., Reylé C., Schultheis M., Picaud S., 2006, *A&A*, 453, 635
- Moffat A. F. J., 1969, *A&A*, 3, 455
- Moorwood A., Cuby J., Biereichel P., et al. 1998, *The Messenger*, 94, 7
- Robin A. C., Reylé C., Derrière S., Picaud S., 2003, *A&A*, 409, 523
- Rousset G., Lacombe F., Puget P., et al. 2003, in P. L. Wizinowich & D. Bonaccini ed., *Society of Photo-Optical Instrumentation Engineers (SPIE) Conference Series Vol. 4839 of Society of Photo-Optical Instrumentation Engineers (SPIE) Conference Series, NAOS, the first AO system of the VLT: on-sky performance*. pp 140–149
- Schlegel D. J., Finkbeiner D. P., Davis M., 1998, *ApJ*, 500, 525
- Skrutskie M. F., Cutri R. M., Stiening R., Weinberg M. D., Schneider S., Carpenter J. M., Beichman C., Capps R., Chester T., Elias J., et al. 2006, *AJ*, 131, 1163
- Stairs I. H., 2004, *Science*, 304, 547
- Stairs I. H., Manchester R. N., Lyne A. G., Kaspi V. M., Camilo F., Bell J. F., D’Amico N., Kramer M., Crawford F., Morris D. J., Possenti A., McKay N. P. F., Lumsden S. L., Tacconi-Garman L. E., Cannon R. D., Hambly N. C., Wood P. R., 2001, *MNRAS*, 325, 979
- Stetson P. B., 1987, *PASP*, 99, 191

- Tam C. R., Stairs I. H., Wagner S., Kramer M., Manchester R. N., Lyne A. G., Camilo F., D'Amico N., 2010, MNRAS, p. 850
- Tauris T. M., van den Heuvel E. P. J., 2006, Formation and evolution of compact stellar X-ray sources. pp 623–665
- Taylor J. H., Cordes J. M., 1993, ApJ, 411, 674
- Thorne K. S., Zytlow A. N., 1975, ApJ, 199, L19
- van Kerkwijk M. H., Bassa C. G., Jacoby B. A., Jonker P. G., 2005, in Rasio F. A., Stairs I. H., eds, Binary Radio Pulsars Vol. 328 of ASP Conference Series, Optical studies of companions to millisecond pulsars. ASP, p. 357
- Zacharias N., Finch C., Girard T., et al. 2010, AJ, 139, 2184